TECHNIQUES FOR CORROSION QUANTIFICATION

GERALD S. FRANKEL

Fontana Corrosion Center, The Ohio State University, Columbus, OH, USA

INTRODUCTION

Corrosion is the deterioration of a material as a result of interaction with its environment. Much of the field of corrosion is focused on the corrosion of metals. However, nonmetals can also suffer environmental degradation. For instance, the ceramic bricks lining a ladle can be attacked by molten steel or a polymer can experience chain scission from ultraviolet radiation. The latter phenomenon can directly affect metal corrosion because polymeric coatings (paints) are widely used to protect metals from the environment. Despite the degradation experienced by all classes of materials in some environments, metallic corrosion is the most important form and the most widely studied. This article will focus on techniques for quantification of metallic corrosion.

Corrosion is so widespread because most metallic materials of practical significance are chemically metastable. Therefore, nature provides the inherent tendency and driving force for the material to revert to its most stable thermodynamic state, which could be, for example, an oxide, hydroxide, sulfide, carbonate, or chloride. Thus, the corrosion scientist and engineer must constantly battle with nature to preserve the metastability of the metallic material for the duration of the component lifetime. Herein lies their major challenge.

The direct economic impact of corrosion has been estimated by many studies. The latest study, published in 2001, estimated the annual economic cost of corrosion in the United States to be $279 billion, or 3.2% of the gross domestic product (CCT, 2001). In addition to these direct costs, the indirect costs associated with corrosion, resulting from factors such as lost productivity, were conservatively estimated to be equal to the direct costs. Clearly, if devices and components can be made from cheaper materials with the same corrosion resistance, or if their lifetimes can be extended, enormous savings are possible.

Accurate measurement of corrosion is essential to predict the life of critical metallic components in service. Corrosion measurement also becomes very important in evaluating the effectiveness of corrosion control strategies. The techniques used to measure corrosion vary depending on whether one is dealing with gas phase corrosion or liquid phase corrosion. Electrochemical techniques, which are a focus of this chapter (see Electrochemical Techniques), are applicable specifically to corrosion occurring in liquid media. Corrosion can be either general or localized. Much of the discussion in this article will focus on the phenomenon of general or uniform loss from metallic surfaces. When a metal corrodes in a liquid, the corrosion can involve a direct dissolution of the metal into the liquid, the conversion of the metal into an inorganic corrosion product layer on the surface, or a combination of both reaction layer formation and dissolution.

In the following sections, electrochemical and nonelectrochemical techniques are described for the quantification of corrosion processes in liquid systems. The electrochemical techniques rely on a fundamental understanding of the corrosion electrochemistry. Taking advantage of the capability of modern electronics to measure small currents, the electrochemical techniques are very sensitive, and often take relatively little time to accomplish. In comparison, the nonelectrochemical techniques are simpler and have broader applicability, but usually have lower sensitivity so that longer test times are required to make reliable measurements. Whereas electrochemical methods typically require a bulk conductive electrolyte for testing, nonelectrochemical methods can be used in gaseous environments or relatively nonconducting liquids.

NONELECTROCHEMICAL TECHNIQUES

A number of nonelectrochemical measurement techniques can be used to assess corrosion rate. Weight loss measurement, considered by some to be the "gold standard" of corrosion testing, is certainly the easiest. ASTM G31 describes a standard practice for immersion testing (ASTM, 2000c). The corrosion rate is given by the mass change normalized by the exposed area and exposure time. A typical unit might be mg/dm^2 per year. This unit is often converted using appropriate constants to thickness change per unit time such as millimeters per year or, in the United States, mils per year (mpy, where a mil is a thousandth of an inch). However, there are important issues to consider even for weight loss measurements. First, because mass can be measured easily only to about 0.1 mg, the sensitivity of weight loss measurements is limited. Other issues include end-grain attack leading to different corrosion rates on different exposed faces, crevice corrosion associated with hanging or supporting the sample, and liquid/air interface or waterline attack if the sample is partially immersed in a liquid. Finally, weight loss measurements are usually performed after long exposure times, so they provide an average rate over time as well as over the exposed surface. They therefore do not capture the slowing of corrosion with time that often occurs, or localization of the attack on the surface. It should be noted that the quartz crystal microbalance can provide rapid and very sensitive (submonolayer) measurements of weight loss for thin film samples (Frankel and Rohwerder, 2003).

Corrosion rate also can be determined by dimensional changes of the exposed samples or analysis of the solution for dissolved species. Both of these approaches also have sensitivity limitations similar to weight loss. However, solution analysis can be particularly powerful for studying the corrosion of alloys because of the ability for chemical differentiation, which is only possible using electrochemistry by rotating ring–disk measurements. A recent approach has shown how atomic emission

Characterization of Materials, edited by Elton N. Kaufmann.

spectroscopic measurements of solution exposed to a sample in a flow cell can be synchronized with linear sweep voltammetry to determine speciation of dissolved material as a function of applied potential (Ogle et al., 2009).

A technique that has had more application in corrosion rate monitoring than in corrosion science involves the change in electrical resistance (ER) of a probe sample. The reduction of the cross-sectional area, A, of a probe by corrosion is accompanied by a proportionate increase in the electrical resistance, R, of the sensing element:

$$R = \rho L/A \quad (1)$$

where ρ is resistivity of the metal and L is the length along which the resistance measurement is made. Commercially available probes allow monitoring of the resistance of the sensing element, which is compared to the resistance of an element of the same material at the same location and temperature that is not exposed to the environment to account for temperature effects on resistivity. The temperature-corrected change in resistance therefore directly reflects the change in cross-sectional area (not exposed area) resulting from metal lost by corrosion. A major advantage of the ER technique is its applicability to a wide range of corrosive conditions including environments having poor conductivity or noncontinuous electrolytes such as vapors and gases. However, ER monitoring typically requires a relatively long exposure period for a detectable difference in probe resistance and electrically conductive deposits can affect the measurements. A comparison of weight loss, ER, and polarization resistance measurements in cooling water applications found that, with increasing extent of localized corrosion, ER measurements indicated corrosion rates in excess of those observed on the coupon (Thierry et al., 1987). In addition, changes in corrosivity of the water systems could be detected within a few hours by the polarization resistance techniques described below, whereas the ER technique required a few days to measure the changes.

The nature of the test depends on the details of the service exposure conditions. Atmospheric exposure conditions are often not well understood or controlled. The electrolyte responsible for atmospheric corrosion can be a thin layer in equilibrium with humid air and influenced by atmospheric pollutants or surface contamination from sources such as road salt. In outdoor exposure, dew and precipitation play a major role in determining the local environment. Time of wetness, defined as the time with $T > 0^{\circ}$C and relative humidity (RH) >80%, has been shown to be a critical parameter for outdoor atmospheric corrosion (Knotkova-Cermakova and Barton, 1982). However, wet layers can exist on contaminated surfaces at much lower values of RH owing to deliquescence of the salts on the surface (Leygraf and Graedel, 2000).

As a result of the complexity of the atmospheric corrosion environment, testing conditions are usually less connected to real exposures. The most common atmospheric exposure test is ASTM B117 salt spray (ASTM, 2000b). However, the relevance of salt spray test performance to real environments, including marine environments, has been discussed widely. In fact, the introduction section of the B117 standard states (ASTM, 2000b): "Prediction of performance in natural environments has seldom been correlated with salt spray results when used as stand alone data. Correlation and extrapolation of corrosion performance based on exposure to the test environment provided by this practice are not always predictable. Correlation and extrapolation should be considered only in cases where appropriate corroborating long-term atmospheric exposures have been conducted." Various cyclic tests have been suggested to be more representative (Haynes, 1995). Microelectronic devices are often tested under conditions of high temperature and humidity (T/H) with the added application of a bias (Frankel and Braithwaite, 2002). The prediction of lifetime in service from lifetime in more aggressive test conditions requires knowledge of acceleration factors. The acceleration factors for microelectronic devices in T/H testing have been studied in some detail (Frankel and Braithwaite, 2002), but acceleration factors for most corrosion tests relative to atmospheric exposures are not known, although various correlations have been made (Haynes, 1995).

The following sections will describe common electrochemical methods used for the assessment of corrosion rate of metals in bulk aqueous environments: the Tafel technique, linear polarization, and electrochemical impedance spectroscopy. In each section, the principles of the method will be introduced, followed by practical aspects and then problems. Other more advanced electrochemical methods exist, but will not be covered in this review.

TAFEL TECHNIQUE

Principles of the Method

When a metal sample is placed in contact with an aqueous electrolyte solution, charge separation occurs at the interface, resulting in a potential drop on the order of a fraction of a volt across a distance of a few nanometers. This potential drop can be assessed from the voltage (or potential) measured by a voltmeter between the sample and another electrode with a constant potential drop of its own, called a reference electrode. This potential, called the open-circuit potential, free potential, or corrosion potential in the case of a corroding electrode, is determined by the required condition of charge conservation. Charge is neither consumed nor created when the combined rate of all the oxidation reactions (such as metal dissolution to form a dissolved ion) is equal to the combined rate of all of the reduction reactions (including the typical cathodic reactions in aqueous systems, hydrogen evolution and oxygen reduction).

Figure 1 shows how the corrosion potential and corrosion rate, given by the corrosion current density, are determined by the thermodynamics and kinetics of the

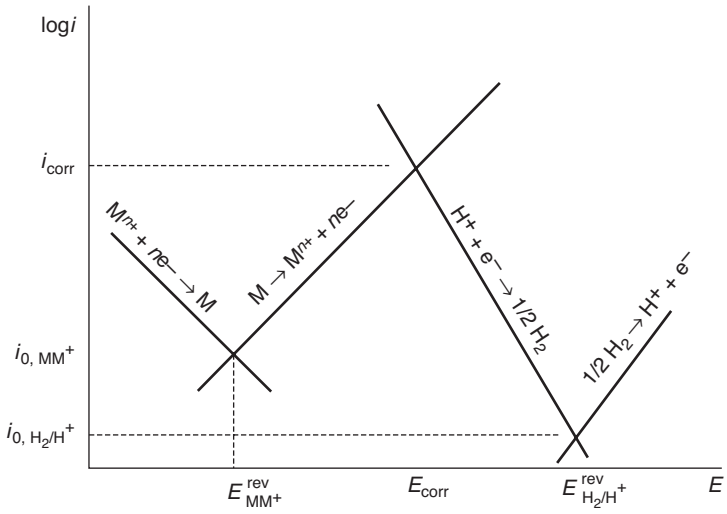

Figure 1. Schematic Evans diagram for corroding active metal in an acid. Reproduced with permission from Frankel and Landolt (2003). Copyright Wiley-VCH.

electrochemical reactions occurring on the surface. In this plot, called an Evans diagram, the *x*-axis is the electrode potential, which is the driving force for the electrochemical reactions, and the *y*-axis is the log of the current density, which is a measure of the rate of the reaction. When the rate-determining step in an electrochemical reaction is the transfer of charge across the interface, so-called activation polarization, there is an exponential relationship between current density and potential such that the electrochemical kinetics can be represented by a straight line in the semilogarithmic plot. On the left side of Figure 1, two straight lines are shown corresponding to the metal oxidation reaction, $M = M^+ + e^-$, and the reverse reaction, metal ion reduction. The intersection of these lines occurs at a point representing the equilibrium electrode potential and the exchange current density of the M/M^+ charge-transfer reaction. Metal oxidation occurs at potentials above the equilibrium potential and metal ion reduction occurs below that potential. For a metal exposed to an aqueous environment, other charge-transfer reactions can occur simultaneously at the metal–aqueous solution interface. In acid solutions, the evolution of hydrogen gas by the reduction of H^+ ions, $H^+ + e^- = {}^1/_2H_2$, is possible. Lines representing the kinetics of the H^+/H_2 oxidation and reduction reactions are shown on the right side of Figure 1. As shown in this figure, the equilibrium potential for the hydrogen evolution reaction is higher (more noble) than that for many metals. The exchange current density for this reaction depends strongly on the catalytic properties of the metal on which it is occurring.

The equation describing the exponential current/potential relationship for the oxidation and reduction of a single-electron half-cell reaction, such as M^+/M and H^+/H reactions given above, for the case of activation polarization is called the Butler–Volmer equation (Bockris and Reddy, 1970):

$$i = i_0\left[\exp\left(\frac{\alpha F(E-E^{rev})}{RT}\right) - \exp\left(-\frac{(1-\alpha)F(E-E^{rev})}{RT}\right)\right] \quad (2)$$

where i is the net rate of the electrochemical half reaction, i_0 is the exchange current density or the rate of both the forward and reverse reactions when an electrochemical half reaction is at equilibrium, E is the electrode potential, E^{rev} is the reversible or equilibrium electrode potential, α is a symmetry factor, F is the Faraday constant, R is the universal gas constant, and T is the absolute temperature. The symmetry factor α, which is typically close to 0.5, describes the portion of the total work associated with moving the charge through the potential drop that affects the activation energy of the forward reaction. The Butler–Volmer equation can be simplified to the following form:

$$i = i_0\left[10^{(E-E^{rev})/b_a} - 10^{(E-E^{rev})/b_c}\right] \quad (3)$$

where b_a and b_c are the Tafel constants that result from the combination of other constants in Equation 2 and a factor to change to base 10. The subscripts a and c indicate the anodic and cathodic or oxidation and reduction directions of the reaction, respectively. If the potential is far enough away from the equilibrium potential, one of the exponential terms in Equations 2 and 3 will dominate, resulting in the Tafel equation, given here for the anodic or oxidation reaction:

$$i = i_0 10^{(E-E^{rev})/b_a} \quad (4)$$

Considering again the situation of a metal sample exposed to an acidic solution so that both metal oxidation and hydrogen evolution can occur, the potential will typically be far enough from both equilibrium potentials that the Tafel equations can be used, thereby disregarding the vanishingly small back reactions. In Figure 1, the intersection of the Tafel line representing the kinetics of the metal oxidation reaction with the Tafel line representing the kinetics of the hydrogen evolution reaction is the point where the rates of those reactions are equal. The requirement for charge conservation at a freely corroding metal sample surface is met at this point. The potential at this intersection is therefore the corrosion or

open-circuit potential. Furthermore, the rate of metal oxidation at the corrosion potential is the corrosion rate, expressed as the corrosion current density. It can be seen that this intersection point describing the corrosion potential and corrosion current density is determined by the kinetics (the Tafel slopes and the exchange current densities) and the thermodynamics (the reversible potentials) of both reactions. This theory, first developed by Wagner and Traud (1938), is often called mixed potential theory because the corrosion potential must lie between the reversible potentials of the primary oxidation and reduction reactions, and is thereby a "mixed" potential.

For a metal sample corroding in an acidic solution, the net current as a function of the electrode potential is given by the difference in the current densities associated with the oxidation and reduction reactions:

$$i = i_{0,\mathrm{M}} 10^{\left(E-E_{\mathrm{M}}^{\mathrm{rev}}\right)/b_{\mathrm{a,M}}} - i_{0,\mathrm{H}} 10^{\left(E-E_{\mathrm{H}}^{\mathrm{rev}}\right)/b_{\mathrm{c,H}}} \tag{5}$$

where M and H in the subscripts represent the M/M^+ and H^+/H reactions, respectively. The net current at the corrosion potential is equal to zero because, for a freely immersed sample, the rate of the metal oxidation reaction has to equal the rate of the hydrogen evolution reaction, a reduction reaction. In other words, at $E = E_{\mathrm{corr}}$, $i_{\mathrm{M}} = i_{\mathrm{H}} \equiv i_{\mathrm{corr}}$, so

$$i_{\mathrm{corr}} = i_{0,\mathrm{M}} 10^{\left(E_{\mathrm{corr}}-E_{\mathrm{M}}^{\mathrm{rev}}\right)/b_{\mathrm{a,M}}} = i_{0,\mathrm{H}} 10^{\left(E_{\mathrm{corr}}-E_{\mathrm{H}}^{\mathrm{rev}}\right)/b_{\mathrm{c,H}}} \tag{6}$$

Solving for $i_{0,\mathrm{M}}$ and $i_{0,\mathrm{H}}$ in terms of i_{corr}, E_{corr}, and E^{rev}, and then replacing in Equation 5, the following expression is obtained for the net current at a corroding metal in an acidic solution as a function of potential:

$$i = i_{\mathrm{corr}} 10^{(E-E_{\mathrm{corr}})/b_{\mathrm{a,M}}} - i_{\mathrm{corr}} 10^{(E-E_{\mathrm{corr}})/b_{\mathrm{c,H}}} \tag{7}$$

This equation is similar in form to the Butler–Volmer equation (Equation 3). It describes the net current for the case of two different oxidation and reduction reactions occurring on a single electrode surface, but both under activation polarization control, whereas the Butler–Volmer equation describes the net current for a single half reaction. There is no agreed-upon name for this equation, but it plays an important role in the field of corrosion as will be described below.

If the potential is controlled at a given value using a potentiostat, as described below, the measured current will be the sum of all the reactions occurring on the surface where oxidation and reduction reactions have opposite polarity. For a potential far above the corrosion potential, the current will be dominated by the oxidation of metal and the measured current will be equal to the rate of metal oxidation. Conversely, if the potential is well below the corrosion potential, the measured current will be dominated by the cathodic reaction. However, at potentials near the corrosion potential, the rates of the oxidation and reduction reaction are of similar magnitude. In fact, at the corrosion potential the two are equal and the net current is zero. Therefore, near the corrosion potential, the measured current deviates from the lines in the Evans diagram representing the Tafel equations for each reaction and goes to minus infinity (log of zero) at the corrosion potential. The bold line in Figure 2 shows the expected measured polarization curve. Note that the absolute value of the current density is plotted because the log of a negative number is undefined. It is implicit in polarization curves that the net current below the corrosion potential is negative.

Figure 2 also shows that straight lines representing Tafel kinetics underlie a measured polarization curve having the form of the bold line. Therefore, extrapolations of the linear Tafel regions of a measured polarization curve should intersect at the corrosion potential. The current density where they intersect represents the corrosion current density. This is the basis of the Tafel technique.

It should be noted that the corrosion current density can be converted into a corrosion rate, r, in moles per second, using Faraday's law:

$$r = \frac{i_{\mathrm{corr}}}{nF} \tag{8}$$

where n represents the valence of the corroding metal (number of equivalents of charge per mole of ions). The corrosion rate R in the engineering unit mpy is given by

$$R = 0.129 \frac{M}{n\rho} i \tag{9}$$

where M is the molecular weight of the metal (g/mol), ρ is the density of the corroding metal (g/cm^3), and i has units of $\mu A/cm^2$.

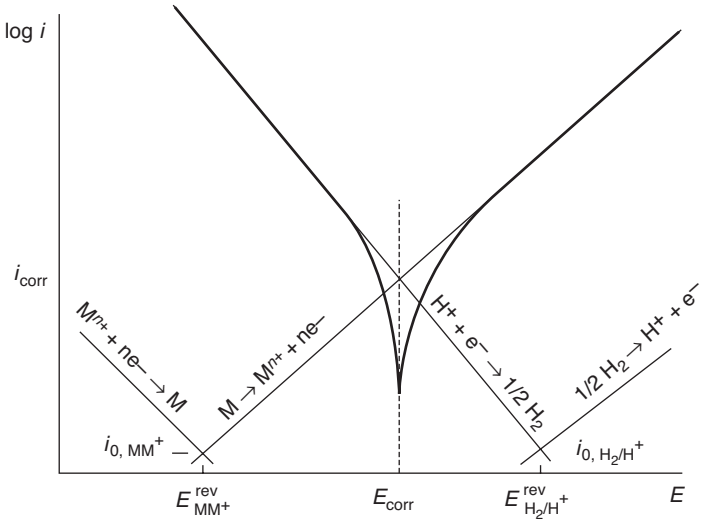

Figure 2. Relationship of measured polarization curve to the Evans diagram for a corroding active metal in an acid. Reproduced with permission from Frankel and Landolt (2003). Copyright Wiley-VCH.

Practical Aspects of the Method

ASTM G5 describes a standard reference test method for potentiodynamic polarization experiments (ASTM, 2000a). A typical electrochemical cell that can be used to measure the corrosion rate of a metal in an aqueous medium is shown in Figure 3 (Jones, 1996). The round bottom glass cell sits in a heating mantle for temperature control if needed. Several electrodes are required for the measurement, including the working electrode, which is the metal under study. A counter electrode or auxiliary electrode is used to pass current to the working electrode. If current were passed through the reference electrode, its potential would change, thereby defeating the purpose of the reference electrode. This electrode should be catalytic and nonreacting, so common materials used for counter electrodes include Pt and graphite. Two counter electrodes are shown in Figure 3. A reference electrode is required to provide a stable reference against which the potential of the working electrode can be measured. A common reference electrode used in corrosion experiments is the saturated calomel electrode (SCE), which has a potential of 0.241 V compared to the thermodynamic reference, the standard hydrogen electrode (SHE). The mercurous sulfate electrode (MSE) can be used if it is critical to keep chloride ions out of the solution. In Figure 3, the reference electrode is located outside the cell with a solution salt bridge connection ending in a Luggin capillary to bring the point of potential measurement close to the working electrode surface, thereby minimizing ohmic potential drops. Also shown in Figure 3 are a thermometer, a glass frit for gas sparging of the liquid, and an exit for the gas. All joints are sealed for gas control.

Preparation of the working electrode is critical because relatively minor details can sometimes have a large effect. The sample is often ground or polished to create a reproducible surface, but the extent of polishing can influence corrosion rate and should be considered carefully. Electrical connection to the sample is required and it is often necessary to limit the exposed area using protective masking material, an epoxy metallographic mount, or some sort of gasket. Alternatively, the sample can be immersed through the waterline with the electrical connection above. The nature of the masking can result in crevice corrosion at the edge of the masking material or waterline attack at the liquid/air interface. All samples should be examined after electrochemical measurements to determine if these forms of corrosion occurred.

Electrochemical measurements are made using electronic instruments called potentiostats, a number of which are commercially available with user-friendly control and data analysis software. A potentiostat contains a control amplifier where one input pole is the desired potential and the other is the potential measured by a high-impedance electrometer between the working and reference electrodes. If the measured and desired potentials are not equal, the control amplifier outputs a current that flows from the counter electrode to the working electrode, thereby altering its potential and setting up a feedback loop. The current is measured by an I/E converter as a potential across a variable resistor. Corrosion experiments are usually performed by scanning the potential at a fixed rate between 0.1 and 1.0 mV/s. The current is measured and the log of the absolute value is plotted as a function of potential.

The Tafel technique requires a clear Tafel region with a linear relation between log i and E over a range of current, preferably at least one order of magnitude. The scan limits must be far enough from the corrosion

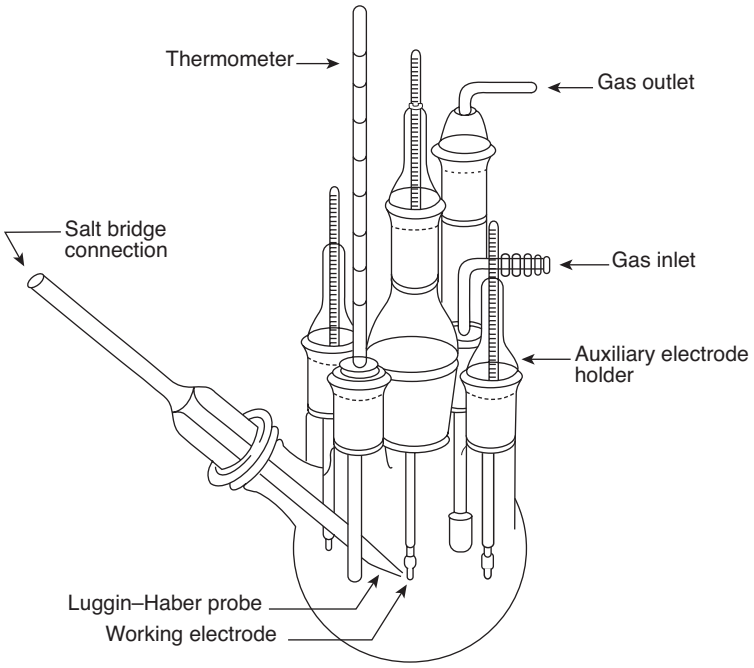

Figure 3. Typical cell for electrochemical corrosion experiments. Reproduced with permission from Jones (1996). Copyright Prentice Hall.

potential to limit the influence of the reaction of opposite polarity. Scanning typically starts in the cathodic region at about 250 mV below the corrosion potential and proceeds upwards through the corrosion potential (or zero-current potential) to a value about 250 mV above the corrosion potential. Because of this requirement to drive the potential far from the natural corrosion potential, this technique is considered to be a "destructive" technique and it is not used for corrosion rate monitoring in the field. Scanning usually starts in the cathodic region because this region typically has less of an influence on the surface of the sample than the anodic region where the sample might dissolve at high rates. In some cases, however, the cathodic polarization has a large influence such that, for instance, the zero-current potential during the upward scan is significantly different than the corrosion potential measured before the scan. In such a case, it is common to perform split scans with the anodic and cathodic portions of the curve measured separately.

An example of a polarization curve measured by potentiodynamic polarization, for the case of Fe in 0.5 M H_2SO_4, is given in Figure 4. In this figure the axes are reversed from those of Figure 1, with the potential on the *y*-axis even though it is the independent variable. This form of plotting is common because of historical reasons. Before potentiostats were readily available, polarization curves were measured by controlling the current and measuring the potential, which is relatively easy to do. The solid line is the measured curve in this plot. The linear portion of the cathodic branch extends for more than a decade of current density allowing accurate manual determination of the Tafel slope, 99 mV/dec in this case. In contrast, the anodic portion of the curve is more complicated, even for this simple system involving Fe dissolution, and a bend in the curve is observed about 75 mV above OCP. The mechanism of iron dissolution to form ferrous ions involves several steps (Landolt, 2007)

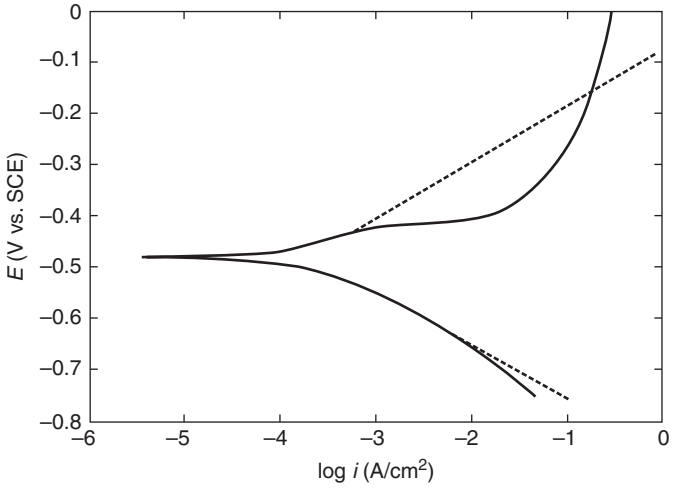

Figure 4. Potentiodynamic polarization curve for Fe in 0.5 M H_2SO_4. Solid line, measured curve; dashed line, fit to Equation 7. Reproduced with permission from Frankel (2008). Copyright ASTM International.

and can change with potential. Determination of the anodic Tafel slope near OCP is difficult owing to the bend in the curve and extrapolation of this region to OCP intersects at a different current density than the extrapolation of the cathodic portion. In such an example, the value of corrosion current density determined by extrapolation of the cathodic region is probably more accurate, 204 $\mu A/cm^2$ in this case. The anodic Tafel slope is determined to be 53 mV/dec by manual fitting.

An alternative and probably more accurate approach is to fit the data to Equation 7, which is the equation representing the net current for metal dissolving in an acidic solution where both reactions are under activation polarization control. The equation therefore represents the form of an ideal polarization curve. Fitting of the data to this equation is similar to Tafel extrapolation except that the data near the corrosion potential are also used in the fit. Nonlinear least-squares fitting of the *i*–*E* data results in determination of the following values: i_{corr}, E_{corr}, b_a, and b_c. A computer is required for such a fit, but experimental data are almost always collected and analyzed by computer these days. Therefore, this approach is certainly more common than Tafel extrapolation. The limits of the fitting must be properly set, however, and in the case of Figure 4 the bend in the anodic curve requires an upper limit of the fit to be quite close to the corrosion potential. The results of the fit, shown as the dashed curve in Figure 4, are anodic and cathodic Tafel slopes of 110 and 103 mV/dec, respectively, and a corrosion rate of 216 $\mu A/cm^2$. At high potentials, the current density becomes independent of potential owing to mass transport limitations and salt film precipitation. Part of the bending of the curve, however, results from ohmic potential drop in solution between the reference and working electrodes. This can be minimized by current interrupt methods, but leads to instability at higher potentials during the onset of passivity.

The potentiodynamic polarization method is used almost exclusively in laboratory investigations. If the corrosion rate was all that one wanted, another technique such as linear polarization, which is described below, would be sufficient. However, the potentiodynamic polarization method provides more information than i_{corr}. As mentioned, the Tafel slopes are determined, and these can be useful for understanding the rate-controlling factors, such as if inhibitors act primarily to block the anodic or cathodic reaction.

Potentiodynamic polarization can also provide information about the ability of a material to passivate at the corrosion potential or at a higher potential and also about the susceptibility of the material to localized corrosion. Figure 5a shows the polarization curve for type 304 stainless steel in 3.5% NaCl solution. This plot is a cyclic polarization curve in which the potential was scanned from the corrosion potential upwards and then at some point the scan direction was reversed. As the potential was increased above the corrosion potential, the current density quickly reached a value of about 10^{-7} A/cm^2 that was independent of potential over a range of several hundred millivolts. It might be considered that this indicates a very large Tafel slope. However,

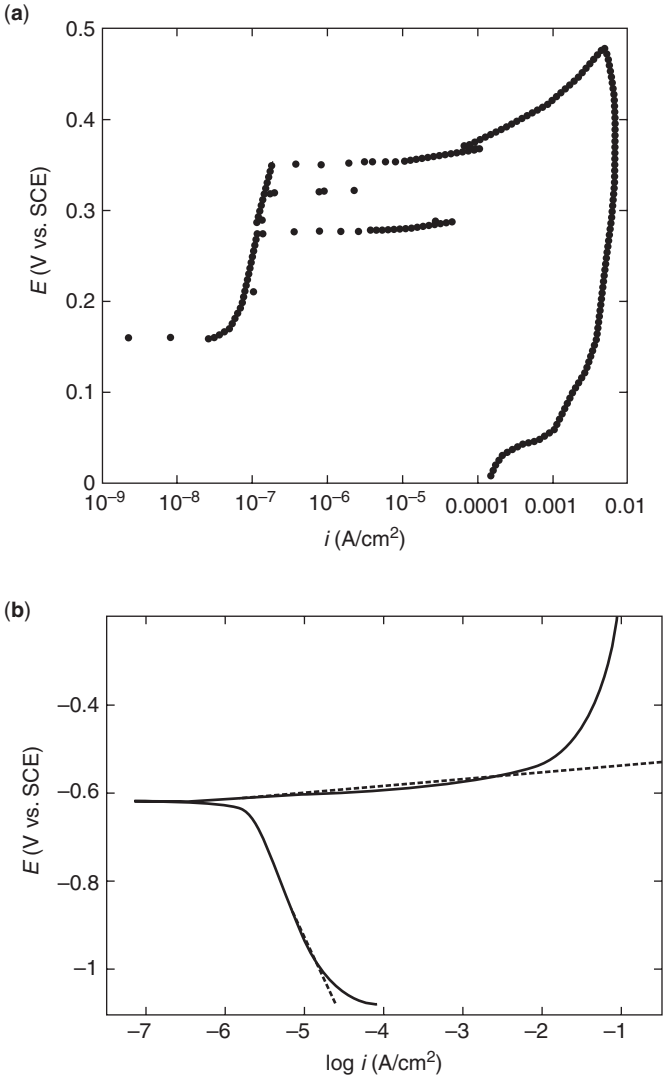

Figure 5. Potentiodynamic polarization curves for (**a**) type 304 SS in 3.5% NaCl and (**b**) AA2024-T3 in 1 M NaCl. Solid line, measured curve; dashed line, fit to Equation 7. Panel b is reproduced with permission from Frankel (2008). Copyright ASTM International.

Tafel slopes should be reserved to describe activation polarization kinetics. In this situation, the low, potential-independent current indicates spontaneous passivation, that is, the presence of a protective thin oxide film that is known to be rich in Cr for the case of stainless steel (Sedriks, 1996). So the potentiodynamic polarization provides information about the tendency of the steel to passivate in this environment. In the passive region of the polarization curve in Figure 5a, current transients or spikes can be seen. These increases in current followed by immediate decreases are evidence of metastable pitting (Frankel et al., 1987), that is, pits that initiate, grow for a short period, and then repassivate. Further increase in potential results in a rapid and sustained increase in current that is associated with the formation of stable pits (Frankel, 1998). The potential associated with the sustained increase in current is called the pitting or breakdown potential (Szklarska-Smialowska, 1986). After the nominal current increased to 5 mA/cm^2 in this experiment, the direction of scanning was reversed and the current during the reverse scan was found to be much larger than that during the upward scan. This hysteresis is evidence that the current increase was associated with a localized corrosion phenomenon such as pitting, crevice, or intergranular corrosion (Szklarska-Smialowska, 1986). It is common for the current to decrease rapidly at some point during the reverse scan, which is indicative of repassivation of the growing pits, and this potential is called the repassivation potential. In the case of Figure 5a, the repassivation potential is below the lowest value reached on the reverse scan. The fact that the repassivation potential is well below the corrosion potential indicates that this alloy is susceptible to crevice corrosion in the test environment. A small hysteresis with repassivation occurring at potentials higher than the corrosion potential would indicate a low susceptibility to localized corrosion.

Figure 5b is the potentiodynamic polarization curve for AA2024-T3 in 1 M NaCl. This curve might be interpreted as representing a material undergoing uniform corrosion with a low anodic Tafel slope. In fact, the dashed line is a fit of Equation 7 to the data. However, this is another case of localized corrosion, but the corrosion potential is pinned at the pitting potential so that pits initiate and grow immediately as the potential is increased above the corrosion potential. If the experiment were repeated in deaerated solution, the corrosion potential would be much lower owing to the absence of dissolved oxygen, which drives up the corrosion potential. In this condition, the polarization curve would look more like that in Figure 5a with a clearly distinguished pitting potential well above the corrosion potential. Samples should be closely examined after every experiment, as described above, for signs of both pitting and crevice corrosion.

Problems

The Tafel technique, performed by either manual extrapolation or fitting of data to Equation 7, is strictly only applicable to the case where both reactions are under activation polarization control, that is, when the rate-determining step is the transfer of charge across the electrode/electrolyte interface. However, there are many practical cases where this is not the case. The cathodic reaction, particularly in aerated neutral environments such as natural environments, is often diffusion-limited oxygen reduction. In that case, the cathodic reaction is rate limiting, so the corrosion rate is given by the rate of oxygen reduction and Tafel extrapolation or fitting is not necessary or appropriate. Similarly, in the case of a spontaneously passive surface, the rate of reaction is limited by passive dissolution. The Tafel technique is not applicable to such cases, but is often used to get a measure of the corrosion rate.

A related problem is that there is often no extended linear region in the semilogarithmic plot to extrapolate from. When neither the anodic nor cathodic branches of

the curve provide a clear Tafel region, extrapolation is not advised, and fitting is equally problematic. In this case, the polarization curves can be compared to assess qualitatively the effects of various factors such as changes in the environment. Ohmic potential drops in solution can be another cause of bending of the polarization curves. Ohmic effects can be minimized by using a Luggin capillary to bring the point of measurement close to the sample surface as shown in Figure 3 and by *IR* compensation methods, although current interrupt *IR* compensation often leads to noise and instability.

In many cases, extrapolations of the anodic and cathodic portions of the curve do not intersect at the zero-current potential, even when extended linear regions exist. In this case it is often considered that the extrapolation of the cathodic branch to the corrosion potential provides a more reliable measure of corrosion rate because lesser change in the sample surface is expected from cathodic polarization than from anodic polarization.

Finally, as mentioned above, this technique is better suited for laboratory investigations than for field monitoring because of the large polarization away from the free corrosion potential that is required.

It should be noted that the corrosion rate for 99.9% Fe in 0.5 M H_2SO_4 determined from the analysis of Figure 4 is about 10× lower than the published rate for steel at room temperature in this concentration (5 wt.%) of sulfuric acid as determined by weight loss measurements, 1200 mpy or 2.5 mA/cm^2 (Fontana, 1957). A corrosion rate of about 200 μA/cm^2 is representative of values measured using electrochemical techniques on Fe in this solution by more than 200 lab groups overseen by the author during lab exercises in university courses and short courses for professionals over the past 15 years. Weight loss measurements performed over the period of days by the same groups typically result in somewhat higher values. These differences between electrochemical and weight loss measurements are interesting and deserve consideration. Electrochemical methods, when interpreted correctly, generate an accurate representation of the instantaneous corrosion rate for the conditions of the measurements. On the other hand, as mentioned above, weight loss measurements are the "gold standard" of corrosion rate measurements and generate an average corrosion rate across the sample surface for the measurement period. These methods might provide different results for various reasons. One difference could be from crystallographic texture. The electrochemical experiments were performed on the sides of a drawn wire or the rolling surface of a plate. During immersion experiments, end-grain attack was observed to be faster than on these surfaces. The rate of attack at the waterline has also been observed to be much higher than the rate well below the surface. This discussion highlights some of the issues associated with corrosion rate testing. Weight loss experiments typically do not differentiate the rates on the different sides of an exposed sample or at a waterline and electrochemical measurements might not be performed on all surfaces or consider waterline attack.

LINEAR POLARIZATION

Principles of the Method

It is possible to determine the corrosion rate of metals in aqueous solutions without polarizing far from the corrosion potential (Mansfeld, 1976). Based on the early work of Wagner and Traud (1938), Stern and Geary (1957) clarified the linear polarization method for determining the polarization resistance, which is inversely related to corrosion rate.

Equation 7 expresses the measured or net current as a function of potential for a metal corroding in an acidic solution. For small values of $E - E_{corr}$, the exponentials can be linearized according to

$$10^{(E-E_{corr})/b} = \exp\left(\frac{E-E_{corr}}{b'}\right) \cong 1 + \frac{dE}{b'} \qquad (10)$$

Note that a modified Tafel slope, $b' = b/2.3$, is used to account for differences in base e and base 10. Using this linearization, the small net current, di, resulting from a small change in potential from E_{corr}, dE, is determined by substituting Equation 10 into Equation 7:

$$\begin{aligned} di &= i_{corr}\, dE\left(\frac{1}{b'_a} - \frac{1}{b'_c}\right) = i_{corr}\, dE\left(\frac{b'_c - b'_a}{b'_a b'_c}\right) \\ &= i_{corr}\, dE\left(\frac{|b'_c| + b'_a}{b'_a |b'_c|}\right) \end{aligned} \qquad (11)$$

The polarization resistance, R_P, is defined as the slope dE/di at the corrosion potential:

$$R_P \equiv \left.\frac{dE}{di}\right|_{E=E_{corr}} \qquad (12)$$

Note that the units of polarization resistance are Ω cm^2. Inserting Equation 12 into Equation 11, the following equation, known as the Stern–Geary equation, is obtained:

$$i_{corr} = \frac{b_a |b_c|}{(b_a + |b_c|)2.3R_P} = \frac{B}{R_P} \qquad (13)$$

where B is a constant that depends on the Tafel slopes. This equation shows that the polarization resistance is inversely proportional to the corrosion rate, which has been proven to be true using nonelectrochemical methods of corrosion rate determination (Stern and Weisert, 1959). For the Stern–Geary approximation to be valid, the applied potential must be within ∼15 mV of the corrosion potential where the linearization is valid. This is a rather general statement; the maximum applied potential to get a linear response depends on the specific corrosion system being investigated. Even if the response is not linear, the tangent at the corrosion potential can be used to determine R_P (Equation 12).

The linear polarization method is very commonly used for corrosion monitoring in field applications because it

requires relatively little potential perturbation from the free corrosion potential and thus can be considered a nondestructive method. However, accurate assessment of corrosion rate by inserting R_P in Equation 13 requires knowledge of the Tafel slopes, which must be measured separately in experiments that do polarize the electrode far from the corrosion potential or found in the literature. Alternatively it is possible to estimate the values of the Tafel slopes without causing a very large error. For example, calculated corrosion rates are usually not wrong by more than a factor of 2–3 if both the Tafel slopes are assumed to be 100 mV/dec. This is often within the scatter of any estimation of corrosion rate.

Practical Aspects of the Method

ASTM G59 describes the standard practice for this method (ASTM, 2000d). The experimental setup for carrying out linear polarization experiments is similar to that described above for the Tafel technique. The main difference is in the voltage range selected. The applied voltages used generally do not extend beyond ±20 mV of the corrosion potential. In this range, in many instances, the potential–current curve is linear. The scan typically starts at a potential below E_{corr} and extends upwards potentiodynamically. The slope, dE/di, at the zero-current potential is a measure of R_P. An easier approach is a two-point measurement at potentials above and below the OCP. Or even simpler, a single measurement can be made at a potential either above or below E_{corr} and the slope dE/di can be determined using the (net current, potential) point of (0, E_{corr}) because the i–E curve must go through this point. These simplified analyses assume that the polarization response is perfectly linear, and error will result if there is any deviation from linearity. The measurement can be automated so that values of R_P are determined at regular intervals to assess the trends in i_{corr} over time.

The linear polarization curve for Fe in 0.5 M H_2SO_4 is shown in Figure 6. In this case, the i–E curve is seen to be quite linear over a range of 40 mV encompassing the corrosion potential. The value of R_P can be determined easily from the slope of the tangent: 107 Ω or 67 Ω cm^2 considering that the exposed area was 0.63 cm^2. This is the same system that was used for the potentiodynamic polarization curve shown in Figure 4. In fact, the linear polarization measurement in Figure 6 was made with the same electrode in the same solution just before the potentiodynamic polarization measurement of Figure 4. Using the values of Tafel slope determined from the fitting of the data in Figure 4 to Equation 7, 110 and 103 mV/dec, and Equation 13, the corrosion rate is estimated to be 345 μA/cm^2, which is about 60% higher than the value determined from the fit of Equation 7 to Figure 4. As mentioned, this is well within the typical scatter of repeated measurements of corrosion rate using any method. If one were to guess that both the Tafel slopes were 100 mV/dec, the estimated value of i_{corr} from Equation 13 would have been 328 μA/cm^2, resulting in little error.

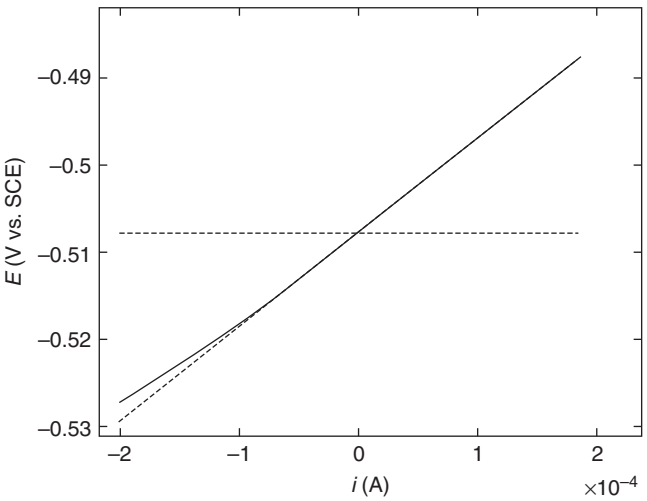

Figure 6. Linear polarization experiment for Fe in 0.5 M H_2SO_4. Tangent is drawn at point where $i = 0$. Reproduced with permission from Frankel (2008). Copyright ASTM International.

Problems

Because the Tafel equations of the oxidation and reduction reactions are the basis for the development of the Stern–Geary equation, a fundamental assumption of the linear polarization method is that both reactions are under activation polarization control. As was the case for the Tafel technique, this method is not strictly applicable for other situations.

Unless *IR* compensation is performed as described above, the ohmic resistance will be an error in the measurement. In fact, the measured polarization resistance, R_P^m, will be the sum of the true polarization resistance, R_P^0, and the ohmic resistance, R_Ω:

$$R_P^m = R_P^0 + R_\Omega \tag{14}$$

The relative error is thus

$$\varepsilon = \left(R_P^m - R_P^0\right)/R_P^0 = R_\Omega/R_P^0 \tag{15}$$

This value will be large when the ohmic resistance is large and the polarization resistance is small. Luckily, in most cases, the corrosion rate is low in resistive media, so this error is usually not large. However, for a case such as the corrosion of iron in ethanolic solutions containing HCl, the error is quite large (Mansfeld, 1976) and *IR* compensation or separate measurement of the solution ohmic resistance is appropriate.

As mentioned above, accurate evaluation of i_{corr} from R_P requires knowledge of the Tafel slopes, but determination of the Tafel slopes by polarizing the electrode far from the rest potential negates one of the advantages of the linear polarization method. Mansfeld (1973) described an approach to estimate the slopes from the linear polarization data. The i–E relationship in Equation 7 is valid near the corrosion potential where the linear polarization measurement is made. As described

above, fitting of this curve to *i*–*E* data generated by potentiodynamic polarization results in determination of four parameters. Actually, the value of E_{corr} is easily determined, so there are really only three unknowns. This can be reduced to two by insertion of Equation 13 into Equation 7 to get

$$i_{net} = \frac{b_a|b_c|}{(b_a+|b_c|)2.3R_P} \times \left[\exp\left(\frac{2.3(E-E_{corr})}{b_a}\right) - \exp\left(\frac{2.3(E-E_{corr})}{b_c}\right)\right] \quad (16)$$

In this equation, the *i*–*E* data can be fitted using only the Tafel slopes as unknowns. The error in this fit is small even using data only over a limited range around E_{corr}. The Tafel slopes can then be inserted into the Stern–Geary equation (Equation 13) to get the corrosion current density.

ELECTROCHEMICAL IMPEDANCE SPECTROSCOPY

Principles of the Method

Electrochemical impedance spectroscopy (EIS, see Electrochemical Impedance Spectroscopy) is a powerful technique for the study of corrosion behavior. Details of the method can be found in several good books and articles (Lorenz and Mansfeld, 1981; Kendig and Mansfeld, 1983; Baboian, 1986, 1995; Macdonald, 1987; Tait, 1994; Cottis et al., 1999). EIS involves the application of a voltage waveform that typically is sinusoidal in nature and measurement of the current response. If the voltage amplitude is low enough that the system is linear (a typical amplitude is 10 mV), the current response will also be a sine wave of the same frequency but offset in phase. If the potential input is

$$E(\omega, t) = E_{mean} + V_0 \sin(\omega t) \quad (17)$$

where E_{mean} and V_0 are the mean value and amplitude of the voltage, respectively, and ω is the radial frequency, then the current output will be

$$I(\omega, t) = I_{mean} + I_0 \sin(\omega t + \theta) \quad (18)$$

where I_{mean} and I_0 are the mean value and amplitude of the current response, respectively, and θ is the phase lag. The relationship between voltage input and current response is shown in Figure 7. If $E_{mean} = E_{corr}$, then $I_{mean} = 0$. The impedance, $Z(\omega)$, is a function of frequency and is given by the ratio of the potential and current signals:

$$Z(\omega) = E(\omega, t)/I(\omega, t) \quad (19)$$

In general, the impedance is a complex number that is characterized by a pair of numbers: either the magnitude, $|Z|$, and the phase shift, θ, or the real, Z', and imaginary, Z'', components, where

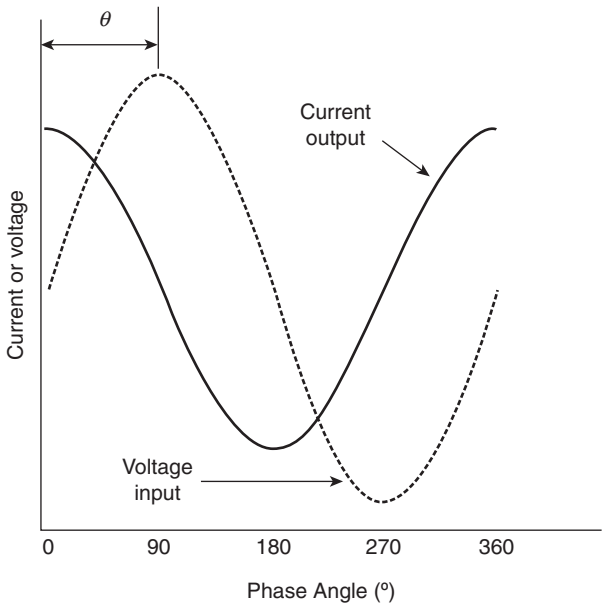

Figure 7. Representation of voltage input, current output, and phase lag, θ, for EIS experiments.

$$Z(\omega) = \text{real} + \text{imaginary} = Z'(\omega) + jZ''(\omega) \quad (20)$$

where $j = \sqrt{-1}$. The voltage input is applied over a range of frequency ($f = 2\pi\omega$), typically from 10^5 to about 10^{-2} to 10^{-3} Hz and the impedance is determined at each frequency. The impedance response is typically modeled using equivalent electrical circuits using passive circuit elements such as resistors, capacitors, and inductors. An electrical circuit that reproduces the response of many electrochemical systems is the simplified Randles circuit, which is shown in Figure 8. The parallel combination of a polarization resistance and double-layer capacitance, C_{DL}, which represents the response of the interface, is in series with the ohmic resistance of the solution between the working and reference electrodes. In many cases, electrochemical interfaces exhibit a nonideal capacitance, so a constant phase element (CPE) is

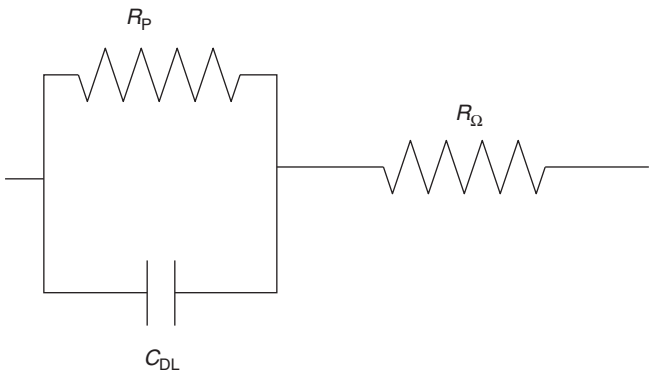

Figure 8. Simplified Randles circuit, which reproduces the response of many electrochemical interfaces.

used instead of a capacitance in the circuit. The CPE is a mathematical construct with impedance given by

$$Z_{CPE} = \frac{1}{A(j\omega)^{\alpha}} \quad (21)$$

where A is the CPE magnitude (with units $\Omega^{-1}\,cm^{-2}\,s^{\alpha}$) and $0 < \alpha < 1$ is a dimensionless exponent that is usually close to 1. If $\alpha = 1$, the CPE acts as an ideal capacitor ($Z_{cap} = 1/j\omega C$), whereas if $\alpha = 0$, the CPE is a resistor ($Z_{res} = R$). In general, the use of CPEs instead of capacitors results in better fitting of the data. The capacitance is not equivalent to the CPE magnitude A, but can be derived from it using (Hsu and Mansfeld, 2001)

$$C_{eq} = A(\omega''_m)^{\alpha-1} \quad (22)$$

where ω''_m is the frequency at which the imaginary component of the impedance is a maximum.

Probing of the electrochemical system over a range of frequency provides more information than the Tafel and linear polarization techniques, which as DC measurements only provide information about the steady-state behavior, or R_P. EIS provides information about R_P, C_{DL}, and R_Ω. R_P measured by EIS can be inserted in the Stern–Geary equation (Equation 13) to get i_{corr} and the capacitance can be used to obtain information about films. Furthermore, clear differentiation of the polarization and ohmic resistances eliminates the issues associated with ohmic potential drops described above for the other techniques, so the technique is well suited for low conductivity applications such as nonaqueous electrolytes, or corrosion of rebar in concrete.

EIS also provides important information about coated samples that is not accessible from the other methods. Figure 9 shows an equivalent circuit that is commonly used to model systems with defective coatings. It is a nested two time constant circuit containing CPEs instead of capacitors. In this circuit, CPE_{FILM} represents the capacitance of the defective film and R_{PORE} represents the ohmic resistance of the pores in the film. The combination of CPE_{DL} and R_P represents the behavior of the metal at the bottom of the pores in the film. By fitting impedance spectra of a coated sample to such a circuit, information about the coating and its defects can be assessed. EIS is particularly powerful for early assessment of coating degradation.

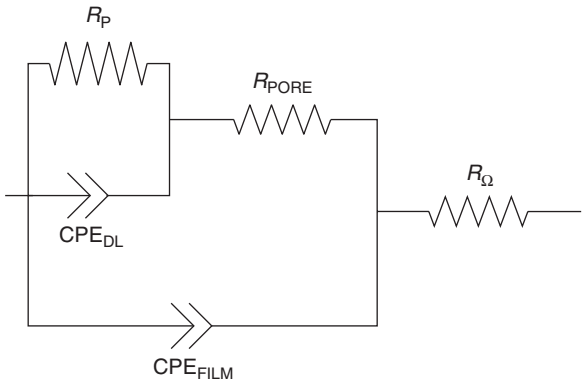

Figure 9. Typical equivalent circuit for a defective coating using CPEs instead of capacitors. Reproduced with permission from Frankel (2008). Copyright ASTM International.

EIS data can be plotted in several ways. Figure 10 shows the two most common plots used for displaying corrosion EIS data. The data are shown as points and the lines are fits to the equivalent circuit shown in Figure 8, except that a CPE was used in place of C_{DL}. The Nyquist plot in Figure 10a is a complex plane plot with $-Z''$ plotted against Z'. Each data point represents a different frequency, which is not explicitly shown in this plot. The data take the form of a semicircle with the lowest-frequency data at the right side and the highest-frequency data on the left side of the semicircle. The high-frequency intercept of the semicircle with the real axis (the x-axis) is R_Ω in Figure 8 and the semicircle diameter is R_P, so the low-frequency intercept is equal to $R_P + R_\Omega$. Data exhibiting a second time constant would show a second semicircle in the Nyquist plot.

Figure 10b is a Bode plot of the same data with the log of the impedance magnitude and the phase shift plotted in separate plots versus the log of the frequency. In the Bode magnitude plot the high-frequency value on the right is R_Ω and the low-frequency value on the left is $R_P + R_\Omega$.

Practical Aspects of the Method

ASTM G106 describes a standard practice for electrochemical impedance measurements (ASTM, 2000e). EIS experiments are typically performed in the same electrochemical cells as those used for the other electrochemical techniques. Modern potentiostats are all capable of performing the experiment and powerful software is available for analyzing the data. A frequency response analyzer (or alternatively a lock-in amplifier) is an extra component of the EIS system needed for data analysis, although a software equivalent might be used.

The applied voltage waveform is typically sinusoidal with amplitude of about 10 mV and mean value equal to the corrosion potential if one is interested in obtaining information about the corrosion rate and open-circuit processes. The frequency is stepped typically from the highest frequency, about 10^5 Hz, downward in several steps per decade of frequency to a low frequency of 10^{-3} to 10^{-2} Hz. The lower the frequency, the longer is the time required to obtain each data point.

Data analysis can be performed manually if the simplified Randles circuit shown in Figure 8 is applied. However, accurate analysis requires nonlinear least-squares fitting of the data to the responses of the selected equivalent circuit using a computer.

The data shown in Figure 10 are for the same Fe in 0.5 M H_2SO_4 system used above for the other techniques. EIS is also quite easy with this system, because the low-frequency limit is reached at a frequency of about 1 Hz. By fitting the data to the simplified Randles circuit shown in Figure 8, except using a CPE instead of C_{DL}, the R_P is found to be 107 Ω or 67 Ω cm^2 considering the

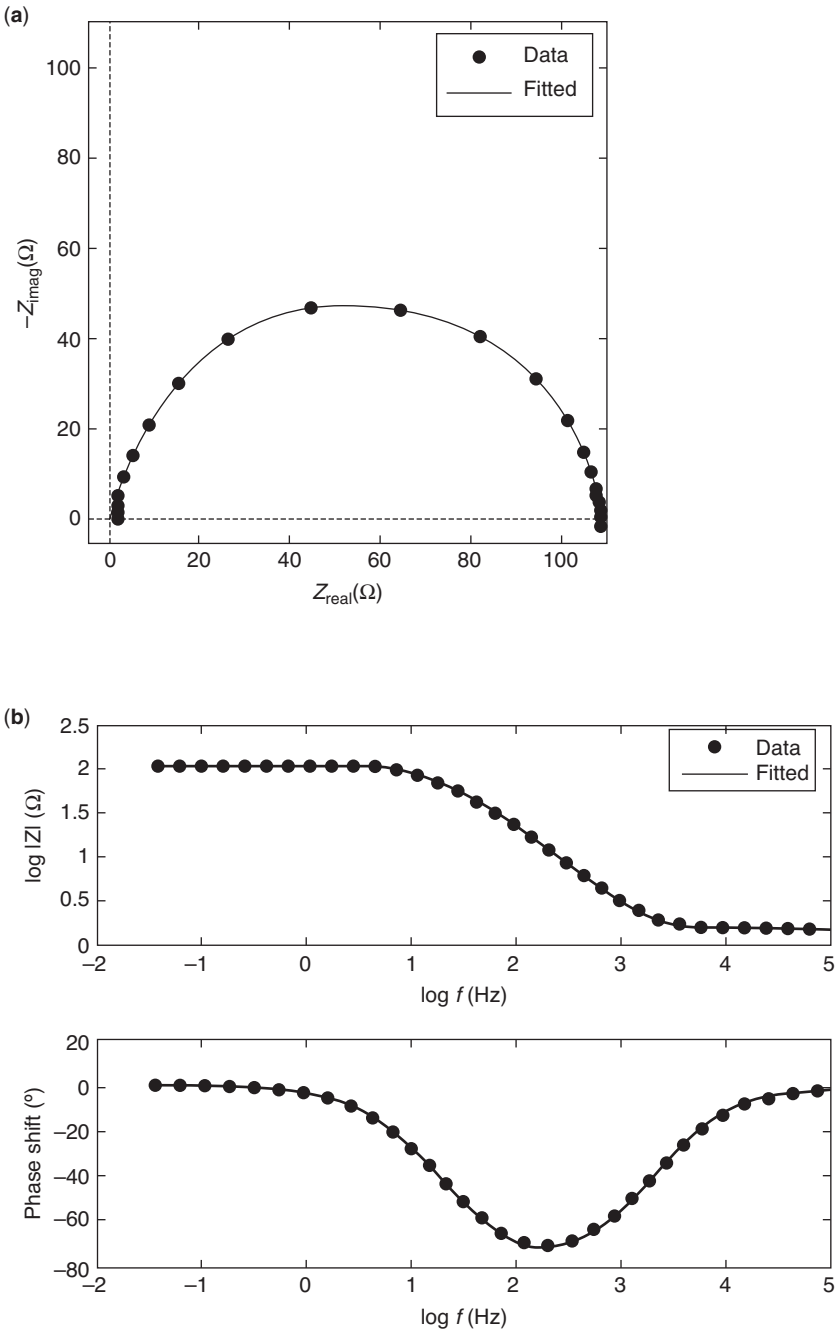

Figure 10. EIS data for Fe in 0.5 M H_2SO_4. (**a**) Nyquist plot and (**b**) Bode plot. The lines are fits to the equivalent circuit shown in Figure 8, except with a CPE instead of C_{DL}.

exposed area of 0.63 cm^2. These values are identical to those determined by linear polarization. As is the case for linear polarization, the calculation of corrosion rate from this value using the Stern–Geary equation requires knowledge of the Tafel slopes, but again the answer will not be much different assuming Tafel slopes of 100 mV/dec.

Problems

EIS is a technique that is no longer difficult to perform owing to user-friendly software, but is particularly susceptible to artifacts and misinterpretations. One main problem is deciding which equivalent circuit to use. The circuits in Figures 8 and 9 are suitable for many corroding systems. Some systems require the addition of diffusional elements, inductors, or transmission lines, the descriptions of which are beyond the scope of this article. However, any equivalent circuit should have a physical model with components that correspond to each element in the circuit. Furthermore, any data can be fitted well if enough fitting variables are added to the model, but the simplest equivalent circuit that can fit the data should be used. At times it is not clear when to add a new time constant. For instance, a time series of measurements to assess the degradation of a coated sample will often start

with spectra showing a single time constant and end with spectra exhibiting two clear time constants. A decision must be made as to when the circuit elements associated with a second time constant are added to the equivalent circuit used in fitting.

As mentioned above, EIS can provide early indication of the degradation of protective coatings such as paint. Changes in the spectra are obvious long before degradation of the paint is visually apparent. A common mistake made by newcomers investigating coated samples is to misinterpret the spectra of protective coatings. Before coating breakdown initiates, a coating will exhibit a purely capacitive response. If the impedance of the coating is higher than the input impedance of the impedance measurement system, then the response will reflect the system properties and not those of the coating. A perfectly reasonable-looking spectrum that can be analyzed using standard equivalent circuits might be produced by the system impedance. It is imperative to know the system impedance, which can be measured using open leads. The connections for every electrode should be allowed to hang in air without touching each other (not placed on a surface) and a complete spectrum should be collected. Any impedance outside of the envelope described by this measurement will be inaccessible by the particular impedance system. Good systems will be able to measure impedance values of about $10^{12}\,\Omega$ at low frequency, but only a much lower impedance at high frequencies owing to the stray capacitance.

For many high-impedance systems with reasonably high capacitance, it is not possible to reach the DC limit (impedance magnitude unchanging and zero phase angle in the Bode plot, or intersection with the real axis in a Nyquist plot) at reasonable frequencies. The data are often quite noisy at frequencies below 10^{-2} Hz, and sometimes unusable. This makes estimation of R_P very difficult, and fits can carry considerable error.

Given the time required to complete a spectrum at low frequencies, very good stability is required. A single measurement at 10^{-3} Hz takes at least 1000 s, so if the corrosion potential is changing by as little as about 1 mV/min, the applied signal will polarize the sample completely away from the corrosion potential by the end of the measurement.

SUMMARY

The techniques described in this article provide an array of approaches to quantify corrosion rate. The nonelectrochemical methods are simple and straightforward. Weight loss measurements provide direct evidence of the corrosion rate. Electrical resistance probes can be used in any environment and are suitable for field monitoring. The electrochemical techniques are based on a fundamental understanding of corrosion kinetics. Tafel extrapolation of potentiodynamic polarization data is a powerful tool for assessing corrosion rate and considerable information beyond the corrosion rate can be determined from the polarization curves. Linear polarization is a simple technique that is widely used in the field to monitor corrosion rates. Knowledge of the Tafel slopes is required for accurate determination of corrosion rate. However, even without knowing the Tafel slopes and thus the corrosion rate, an observation of a change in the polarization resistance during field monitoring can be used to initiate a detailed inspection. EIS is a powerful technique, in particular for corrosion in low conductivity media or under coatings, but it has not yet been widely accepted beyond research laboratories.

BIBLIOGRAPHY

"Electrochemical Techniques for Corrosion Quantification" in *Characterization of Materials*, 1st ed., Vol. 1, pp. 592–604, by T. A. Ramanarayanan, Exxon Research and Engineering Company, Annandale, New Jersey; Published online: October 15, 2002, DOI: 10.1002/0471266965.com051.

LITERATURE CITED

ASTM. 2000a. ASTM G5-94, standard reference test method for making potentiostatic and potentiodynamic anodic polarization measurements. *In* Annual Book of ASTM Standards, Vol. 3.02, p. 57. ASTM, Philadelphia, PA.

ASTM. 2000b. B117-97, Standard Practice for Operating Salt Spray (Fog) Testing Apparatus. ASTM, Philadelphia, PA.

ASTM. 2000c. G31-72, standard practice for laboratory immersion corrosion testing of metals. *In* Annual Book of ASTM Standards, Vol. 3.02, p. 99. ASTM, Philadelphia, PA.

ASTM. 2000d. G59-97, standard practice for conducting potentiodynamic polarization resistance measurements. *In* Annual Book of ASTM Standards, Vol. 3.02, p. 233. ASTM, Philadelphia, PA.

ASTM. 2000e. G106-89, standard practice for verification of algorithm and equipment for electrochemical impedance measurements. *In* Annual Book of ASTM Standards, Vol. 3.02, p. 450. ASTM, Philadelphia, PA.

Baboian, R. (ed.) 1986. Electrochemical Techniques. NACE, Houston, TX.

Baboian, R. (ed.) 1995. Corrosion Tests and Standards. ASTM, Philadelphia, PA.

Bockris, J. O. M. and Reddy, A. K. N. 1970. Modern Electrochemistry. Plenum, New York.

CCT. 2001. Corrosion Costs and Preventive Strategies in the United States, by CC Technologies Laboratories, Inc. to Federal Highway Administration (FHWA), Office of Infrastructure Research and Development, Report FHWA-RD-01-156.

Cottis, R. A., Turgoose, S., Syrett, B. C., Cottis, B., and Newman, R. 1999. Corrosion Testing Made Easy: Impedance and Noise Analysis. NACE, Houston, TX.

Fontana, M. G. 1957. Corrosion: A Compilation. The Press of Hollenback, Columbus, OH.

Frankel, G. S. 1998. Pitting corrosion of metals; a review of the critical factors. *J. Electrochem. Soc.* 145:2186–2197.

Frankel, G. S. "Electrochemical Techniques in Corrosion; Status, Limitations and Needs," *J. ASTM Int.*, 5, Issue 2 (2008) online ISSN: 1546-962X, DOI: 10.1520/JAI101241, http://www.astm.org/JOURNALS/JAI/TOC/JAI522008.htm.

Frankel, G. S. and Braithwaite, J. W. 2002. Corrosion in microelectronic and magnetic data-storage devices. *In* Corrosion

Mechanisms in Theory and Practice, 2nd ed. (P. Marcus, ed.). Marcel Dekker, New York.

Frankel, G. S. and Landolt, D. 2003. "Kinetics," in *Encyclopedia of Electrochemistry*, edited by A. J. Bard and M. Stratmann, *Vol. 4, Corrosion and Oxide Films*, edited by M. Stratmann and G. S. Frankel, pp. 25–49, Wiley-VCH, Weinheim, Germany.

Frankel, G. S. and Rohwerder, M. 2003. Experimental techniques for corrosion. *In* Encyclopedia of Electrochemistry, Vol. 4, Corrosion and Oxide Films (M. Stratmann and G. S. Frankel, eds.), pp. 687–723. Wiley-VCH, Weinheim, Germany.

Frankel, G. S., Stockert, L., Hunkeler, F., and Boeni, H. 1987. Metastable pitting of stainless steel. *Corrosion* 43 (7):429–436.

Haynes, G. S. (ed.) 1995. Cyclic Cabinet Corrosion Testing. ASTM, Philadelphia, PA.

Hsu, C. H. and Mansfeld, F. 2001. Concerning the conversion of the constant phase element parameter Y-0 into a capacitance. *Corrosion* 57:747.

Jones, D. A. 1996. Principles and Prevention of Corrosion. Simon and Schuster, Upper Saddle River, NJ.

Kendig, M. and Mansfeld, F. 1983. Corrosion rates from impedance measurements: an improved approach for rapid automatic analysis. *Corrosion* 39 (11):466–467.

Knotkova-Cermakova, D. and Barton, K. 1982. Corrosion aggressivity of atmospheres (derivation and classification). *In* Atmospheric Corrosion of Metals, ASTM STP 767 (S. W. Dean, Jr. and E. C. Rhea, eds.), pp. 225–249. ASTM, Philadelphia, PA.

Landolt, D. 2007. Corrosion and Surface Chemistry of Metals. EPFL Press, Lausanne.

Leygraf, C. and Graedel, T. E. 2000. Atmospheric Corrosion. Wiley-Interscience, New York.

Lorenz, W. J. and Mansfeld, F. 1981. Determination of corrosion rates by electrochemical DC and AC methods. *Corros. Sci.* 21 (9):647–672.

Macdonald, J. R. (ed.) 1987. Impedance Spectroscopy. John Wiley and Sons, New York.

Mansfeld, F. 1973. Simultaneous determination of instantaneous corrosion rates and tafel slopes from polarization resistance measurements. *J. Electrochem. Soc.* 120: 515–518.

Mansfeld, F. 1976. The polarization resistance technique for measuring corrosion currents. *In* Advances in Corrosion Science and Technology, Vol. 6 (M. G. Fontana and R. W. Staehle, eds.), pp. 163–262. Plenum, New York.

Ogle, K., Baeyens, J., Swiatowska, J., and Volovitch, P. 2009. Atomic emission spectroelectrochemistry applied to dealloying phenomena: I. the formation and dissolution of residual copper films on stainless steel. *Electrochim. Acta* 54 (22): 5163–5170.

Sedriks, A. J. 1996. Corrosion of Stainless Steels. John Wiley and Sons, New York.

Stern, M. and Geary, A. L. 1957. Electrochemical polarization I. a theoretical analysis of the slope of polarization curves. *J. Electrochem Soc.* 104:56.

Stern, M. and Weisert, E. D. 1959. Experimental observations on the relation between polarizatin resistance and corrosion rate. *Proc. Am. Soc. Testing Mater.* 32:1280–1290.

Szklarska-Smialowska, Z. 1986. Pitting Corrosion of Metals. NACE, Houston, TX.

Tait, W. S. 1994. An Introduction to Electrochemical Testing for Practicing Engineers and Scientists. PairODocs Publications, Racine, WI.

Thierry, D., Thoren, A., and Leygraf, C. 1987. Corrosion monitoring techniques applied to cooling water and district heating systems, Paper 463. Corrosion/87, NACE, Houston, TX.

Wagner, C. and Traud, W. 1938. Concerning the evaluation of corrosion reactions by superposition of electrochemical partial reactions and concerning the potential formation on mixed electrodes. *Z. Elektrochem.* 44:391.

KEY REFERENCES

Jones, 1996. See above.

This is a good textbook on all aspects of corrosion.

Kelly, R. G., Scully, J. R., Shoesmith, D. W., and Buchheit, R. G. 2003. Electrochemical Techniques in Corrosion Science and Engineering. Marcel Dekker, New York.

This book provides a detailed description of many electrochemical techniques that are used in corrosion.

Baboian, R. and Dean, S. W. 1990. Corrosion Testing and Evaluation: Silver Anniversary Volume. ASTM, Philadelphia, PA.

Another detailed compilation of corrosion testing, including electrochemical methods.

Cottis et al., 1999. See above.

An approachable book on EIS including fundamentals and practical suggestions.